Eur. Phys. J. D **45**, 539–546 (2007)
DOI: 10.1140/epjd/e2007-00255-9

THE EUROPEAN PHYSICAL JOURNAL D

Magnetic properties of deposited gadolinium atoms, dimers and their monoxides

M. Martins[a], M. Reif, L. Glaser, and W. Wurth

Institut für Experimentalphysik, Universität Hamburg, Luruper Chaussee 149, 22761 Hamburg, Germany

Received 26 January 2007 / Received in final form 11 June 2007
Published online 31 August 2007 –

Abstract. Magnetic properties of gadolinium clusters deposited on magnetic ultrathin Fe/Cu(100) films have been measured using X-ray Magnetic Circular Dichroism spectroscopy (XMCD). $3d \rightarrow 4f$ as well as $4d \rightarrow 4f$ absorption spectra are presented and discussed. Changes in the relative peak intensities between the monomer, dimer and the corresponding monoxides are observed for the $4d \rightarrow 4f$ $^8D_{7/2}$ multiplets. The comparison with bulk measurements and calculations exhibit a transition from atomic like to bulk like properties.

PACS. 75.75.+a Magnetic properties of nanostructures – 75.70.-i Magnetic properties of thin films, surfaces, and interfaces – 75.50.Cc Other ferromagnetic metals and alloys

1 Introduction

Rare earth elements are characterized by their open f shells, giving rise to large magnetic moments. A prominent example of the lanthanides is gadolinium, showing distinct magnetic properties. As one of the four elements being ferromagnetic at room temperature (Fe, Co, Ni, Gd), the electronic ground state of free gadolinium atoms is $[Xe]4f^7 5d^1 6s^2$, consisting of seven unpaired $4f$ electrons ($S = 7/2$, $L = 0$), one $5d$ electron ($S = 1/2$, $L = 2$) and two $6s$ electrons ($S = 0$, $L = 0$). Due to its exactly half filled f-shell and hence, the rather simple electronic structure, gadolinium is an interesting model system for the exploration of its magnetic properties. According to Hund's rules, the spin moment is at maximum and the orbital magnetic moment vanishes for the f-electrons. For free gadolinium atoms, the magnetic moments of the $4f$- and $5d$-electrons couple to a total magnetic moment of 6.53 μ_B; the $6s$-electrons do not contribute to the total magnetic moment, as they couple to zero.

In the case of gadolinium bulk, the situation changes. Direct exchange interaction between the $4f$ electrons of gadolinium and $4f$ orbitals of neighboring atoms can be neglected due to the localized character of the $4f$ electrons. However, the $5d$ and $6s$ valence-electrons are delocalized in bulk-like systems. Therefore exchange coupling of the $4f$ electrons can be mediated by the valence electrons. This interaction gives rise to magnetic ordering in bulk-like systems, as the intra-atomic $4f$-valence exchange induces interatomic magnetic coupling of the localized f states, resulting in a macroscopic magnetization. This type of indirect ferromagnetic ordering ist called Ruderman-Kittel-Kasuya-Yosida exchange interaction (RKKY). For Gd bulk a ferromagnetic ordering is found. However quite complicated magnetic ordering with canted spins is found for some of the other rare earth elements e.g. for Ho or Dy [1].

Due to the fact that there is only one electron in the $5d$ states, its contribution to the magnetic moment is comparably small. A total magnetic moment of 7.55 μ_B per atom [2] is found for gadolinium bulk experimentally and the difference to the free atom value has its origin in a different coupling of the d-electron moments.

High total magnetic moments of gadolinium have been demonstrated by electron-spin-resonance (ESR) measurements for gadolinium dimers in rare gas (Kr, Ar) matrices [3]. Here, the gadolinium dimer shows a ferromagnetic coupling between all unpaired electrons giving rise to an overall magnetic moment of 8.82 μ_B per atom. The magnetic properties of gadolinium depend strongly on the coordination of the Gd-atoms.

In the literature, a discussion on the magnetic properties of the gadolinium (0001) surface is ongoing. Due to breaking of the symmetry at the surface, modified magnetic properties are found for the surface gadolinium layers. In the focus are effects like surface enhanced magnetic ordering (SEMO) [4–9], enhanced Curie temperatures for the surface layer, as well as an interplay between ferromagnetic (FM) [8,10] and antiferromagnetic (AF) [4,5,7, 11] coupling of the surface moments to the bulk moments. As a consequence of the interplay, thermal induced surface spin reorientation transitions [6,12] are found.

These results obviously display interesting open questions in the field of magnetic properties of rare earth

[a] e-mail: michael.martins@desy.de

system and in particular of gadolinium in reduced dimensions. By further reduction of the size and the coordination, as it is for clusters, the effects are expected to become more important. Here, the Gd_{13} cluster has evolved as a model system for Heisenberg calculations of the magnetic properties of free gadolinium clusters [12–15]. To gain insight in the RKKY-type magnetic coupling mechanism, competing ferromagnetic nearest neighbor and antiferromagnetic next-nearest neighbor coupling are modelled. Canted spin configurations in relation to the geometric structure are one of the major issues of these calculations.

These model calculations were stimulated by Stern-Gerlach type experiments for free gadolinium clusters [16–18]. A strong size dependence of the magnetic moments is observed in the clusters, which manifests itself in a strong reduction of the magnetic moments with increasing cluster size. Moments between 2.94 μ_B and 3.88 μ_B per atom are found using a locked moment model (11–30 atoms per cluster [16,17]), and moments between 5.4 and 5.0 μ_B per atom are found by the application of a superparamagnetic model (13, 21, 22 atoms per cluster [18]). To explain these strongly reduced magnetic moments, the authors suggest a non-collinear spin alignment between the $4f$ spin moments at the atomic sites, thereby confirming the model calculations discussed before.

Non-collinear alignment of the atomic spin moments is consistently observed for deposited gadolinium nanoclusters in experimental [19,20] and theoretical studies [21,22]. Here, reduced magnetic moments for particles up to 3 nm are found, and therefore again the magnetic behavior deviates from the bulk-like [21].

We have investigated Gd atoms and dimers and their respective mono-oxides in contact with a ferromagnetic surface to study the influence of atomic coordination and coupling to neighboring atoms on the magnetic properties. In the following we will present results based on X-Ray Magnetic Circular Dichroism (XMCD) measurements of $3d \rightarrow 4f$ and $4d \rightarrow 4f$ absorption resonances.

2 Experimental

The magnetic properties of the cluster samples are accessed using X-ray Absorption Spectroscopy (XAS) utilizing circular polarized X-rays for excitation (XMCD). Its element specifity and ability to determine spin and orbital magnetic moments make it an ideal tool to investigate the magnetic properties of dilute cluster samples.

The gadolinium clusters are produced by high energy ion sputtering using 30 keV Xe^+ ions to erode the cluster material and thereby produce the clusters. To optimize the yield of the sputter process, a high purity gadolinium target (99.9% Goodfellow) is used as target material which prevents the production of impure clusters. The positively charged cluster ions are collected and accelerated by an electrostatic lens system to a kinetic energy of 500 eV. To mass separate the various clusters sizes, the beam is deflected using a magnetic dipole field featuring a resolution of $m/\Delta m \approx 50$. To reduce fragmentation and implantation into the substrate surface during deposition, the clusters are refocused and decelerated down to a kinetic energy 1 eV per atom. In addition, a soft landing scheme [23,24] is used during cluster deposition, where argon condensated onto the sample surface is used as buffer system. This scheme effectively suppresses fragmentation during cluster deposition [25,26]. The argon is desorbed by flash heating to ≈80 K before the measurements and the clusters are thereby directly supported by the substrate surface. The argon layer thickness has been controlled using XPS. A layer thickness of ∼5 ML of argon is used to ensure soft landing conditions.

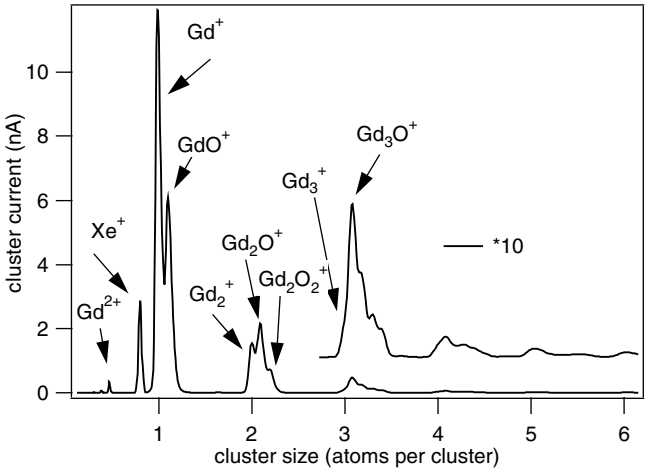

Fig. 1. Mass spectrum of free gadolinium clusters with 500 eV kinetic energy. The clusters can partly be prevented from oxide formation.

Low sample temperatures (∼30 K) are used to inhibit cluster agglomeration and therefore, in combination with low cluster coverages (3% of a monolayer, i.e. $\approx 10^{13}$ atoms/cm^2), the cluster-cluster interaction can be neglected.

The production and mass separation of the clusters is carried out at a base pressure of 1×10^{-8} mbar. The detailed description of the cluster source and its capabilities is given in [27].

A mass spectrum of gadolinium is given in Figure 1. The gadolinium clusters are easily oxidized, therefore only a small size range of the clusters can be separated from their oxides and the yield for larger cluster sizes drops drastically. However, gadolinium monomers, dimers and their monoxides can be separated and have been prepared in this work.

Because the average magnetic properties of many clusters are measured in X-ray absorption spectroscopy ($\sim 10^{11}$ atoms), the magnetic moments of the clusters have to be aligned. This was realized by depositing the gadolinium clusters onto ultrathin remanently magnetized Fe/Cu(100) films. The iron layer thickness was hereby chosen in the range of ∼3–5 monolayers, so that perpendicular magnetic anisotropy [28–30] is observed. Thereby, the direction of the magnetic field can be aligned parallel to the photon helicity in normal incidence geometry. The out of

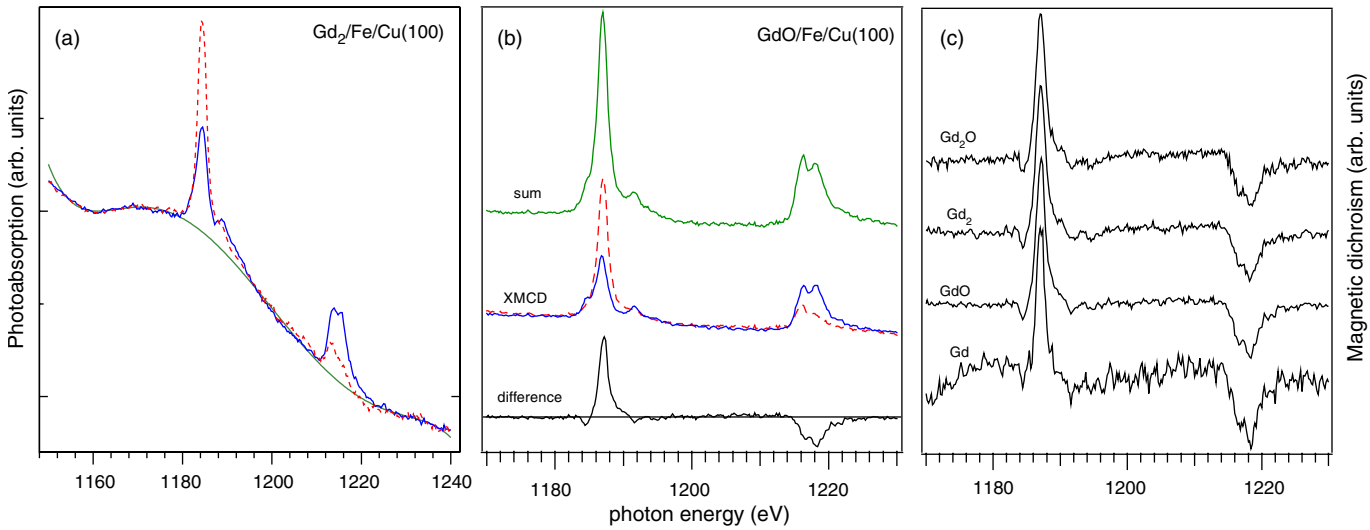

Fig. 2. (Color online) (a) Example of the background subtraction at the Gd $3d$ edges for a Gd_2 sample. The strong variation of the background is due to an EXAFS wiggle of the Fe/Cu(100) substrate. The solid green line is a higher order polynomial, which is fitted to the background outside the Gd resonances. (b) $3d_{5/2,3/2}$ X-ray magnetic dichroism, sum and difference spectra of GdO. (c) $3d \rightarrow 4f$ difference spectra of the Gd, Gd_2 and their monoxides. No change in the spectra for the various clusters is observed.

plane magnetism of the iron films is probed and controlled using XMCD (see below).

All these measurements have been carried out at a base pressure below $p < 2 \times 10^{-10}$ mbar and a sample temperature of 20 K. As a measure for the X-ray absorption, the Total Electron Yield (TEY), in our experiment the total sample current, is recorded.

The experiments have been carried out at beamline UE56/1-PGM and UE52-SGM at the BESSY II storage ring in Berlin and the cluster samples have been prepared in situ at the synchrotron. The $4d \rightarrow 4f$ spectra are measured in an energy range of 135 to 160 eV with a step width and a beamline resolution of 200 meV. A counting time of 4 s per data point has been used for each photon helicity. The beamline resolution for the $3d \rightarrow 4f$ spectra and the step width was set to 300 meV. An energy range of 1170 to 1240 eV and 4 s counting time per data point have been used for the measurements.

For extracting the magnetic properties from the measured spectra, the following data treatment has been applied for both, the $3d \rightarrow 4f$ and $4d \rightarrow 4f$ XMCD spectra. For the normalization on the incident photon flux, the cluster spectra have been divided by reference spectra of the refocussing mirror. To account for the background of the dilute cluster samples, cluster free spectra in the energy region of the gadolinium absorption have been measured. Subsequently, the cluster spectra are divided by these background spectra. Subtraction is in this case less applicable [31] and therefore the results presented in this work are determined from the spectra corrected for by division. Difference and sum spectra are generated by subtraction and addition of the spectra measured with different photon helicity. A straight line has been fitted to and subtracted from the difference and sum spectra to remove a drift. Normalized dichroism spectra of the $4d \rightarrow 4f$ spectra are generated by normalizing the difference spectra onto the sum spectra of each cluster preparation.

The magnetism of the Fe films supporting the clusters has been monitored by recording Fe $2p \rightarrow 3d$ XMCD spectra. A standard procedure for the data evaluation has been used, including the subtraction of a double-step function with a 2:1 step ratio. Applying XMCD sum rules, average values for the spin magnetic moments of $m_s = 1.9 \pm 0.1\ \mu_B$ and for the orbital magnetic moments of $m_o = 0.06 \pm 0.04\ \mu_B$ are found. Here, the magnetic moments have been corrected for a degree of polarization of the circular polarized photons of 90% and the number of d-holes set to $n_h = 3.4$ [32,33]. The spin magnetic moments are found to be stable for the various preparations.

3 Results and discussion

At first, the results of the measurements at the gadolinium $3d$ absorption edges will be presented and discussed. The $3d$ core electrons are mainly excited into unoccupied $4f$ states, as the radial matrix element of the $3d \rightarrow 6p$ excitation is small compared to the $3d \rightarrow 4f$ excitation. Therefore, the properties of the unoccupied $4f$ states are probed in this absorption experiment. Figure 2b shows XMCD spectra of the gadolinium $3d_{3/2,5/2}$ resonances of GdO deposited onto the iron surface. The corresponding sum (top) and difference spectra (bottom) are appended to the graph. In these spectra the main features consist of the two maxima of the spin-orbit split $3d_{5/2,3/2}$ core levels. Figure 2c shows difference spectra of Gd, GdO, Gd_2 and Gd_2O. The sign of the $3d_{5/2}$ and $3d_{3/2}$ areas in the difference spectra are the same. This observation has its origin in the coupling to the iron underlayer and means that the moments of the various gadolinium samples couple in the same way to the iron substrate. Comparing iron

$2p \rightarrow 3d$ asymmetries with the asymmetries of the gadolinium $3d \rightarrow 4f$, the sign of the $2p_{3/2}$ and $3d_{5/2}$ as well as $2p_{1/2}$ and $3d_{3/2}$ areas are opposite in the dichroism spectra. This behavior is a result of an antiferromagnetic coupling between the cluster magnetic moments and the iron layers. The antiferromagnetic coupling observed refers to the coupling between the Gd $4f$ and Fe $3d$ magnetic moments. The antiferromagnetic coupling between magnetic moments of iron and rare earth elements is well-known from experiments [34–36] and originates from spin dependent hybridization. This effect is well described by the model of Brooks and Johansson [37,38]. However, coupling between the support and a cluster could be different, but our experimental results show clearly anti-ferromagnetic coupling.

Sum spectra generated from the spectra measured with circular polarized photons are comparable to spectra measured with linear polarized light with the direction of the electric field vector oriented parallel to the substrate surface. Comparing the sum spectra of the cluster preparations with each other, no difference within these spectra is observed. In addition, the comparison of the cluster spectra with XA spectra of gadolinium bulk [39] gives again no qualitative difference in the shape and structure of the gadolinium $3d \rightarrow 4f$ absorption spectra.

The major difference in the electronic structure between free atoms, clusters and bulk is the increasing delocalization of the $(5d6s)^3$ valence states for bulk-like systems and changes between deposited atoms, clusters and bulk are expected, whereas the structure of the localized $4f$ states remain unaffected. The strong similarity between $3d \rightarrow 4f$ cluster and bulk spectra indicates a negligible influence of a change in the $(5d6s)^3$ valence states on the $4f$ states. This behavior is approved by a comparison with europium $3d \rightarrow 4f$ XA spectra [39]. Generally, europium is an interesting model system for the understanding of the electronic, and thereby the magnetic, properties of gadolinium, as its electronic ground state is $[\mathrm{Xe}]4f^7 6s^2$ and the only difference between europium and gadolinium free atoms is the missing $5d$ electron for europium. The comparison of the shape of europium and gadolinium XA bulk spectra shows no difference for the $3d_{5/2,3/2}$ resonances. Thus, the absence of the $5d$ electron, as an extreme case of a change in the $(5d6s)^3$ valence states, has no impact on the shape of the $3d \rightarrow 4f$ absorption spectra and therefore on the properties of the $4f$ states.

Therefore, as a first result we can conclude from the sum spectra, that the electronic structure of the $4f$ states is not affected by changing the $5d$ occupancy, because no change is observed in the peak positions, the peak shapes or the relative intensities for the different prepared clusters as compared to bulk or surface spectra.

Figure 2c shows $3d \rightarrow 4f$ dichroism spectra of the prepared gadolinium samples. The height of the $3d_{5/2}$ maximum is set to one, to visualize changes in the various samples. Here, no qualitative and quantitative changes between gadolinium monomers and dimers are observed in the $3d \rightarrow 4f$ dichroism spectra. In addition, monoxide formation leaves the spectral properties unchanged within the statistical limits. This null effect can be understood by a close look to the cluster-substrate interaction. Due to their strong localization, no relevant overlap between the $4f$ orbitals and orbitals of surrounding atoms is present. Therefore it is expected that their properties, in particular the magnetic ones, remain unchanged within a change of the coordination or oxidation state. The alignment of the $4f$ magnetic moments is maintained via the indirect RKKY-type exchange coupling. Here, the $5d$ electrons mediate the interatomic exchange coupling between the iron $3d$ and gadolinium $4f$ electrons. The gadolinium $5d$ electrons are expected to be strongly influenced by the surrounding of the gadolinium atoms, as the d electrons are strongly delocalized in bulk-like systems. The rising delocalization of d-electrons has been shown in another investigation [41] for small deposited clusters of the transition metal chromium. To sum up, the identity of the $3d \rightarrow 4f$ dichroism for the investigated gadolinium systems is expected, as the $4f$ magnetism is not influenced by the surrounding. The coupling to the iron substrate does not, beside the magnetic alignment due to the exchange coupling via the $5d$ electrons, influence the $4f$ magnetic properties.

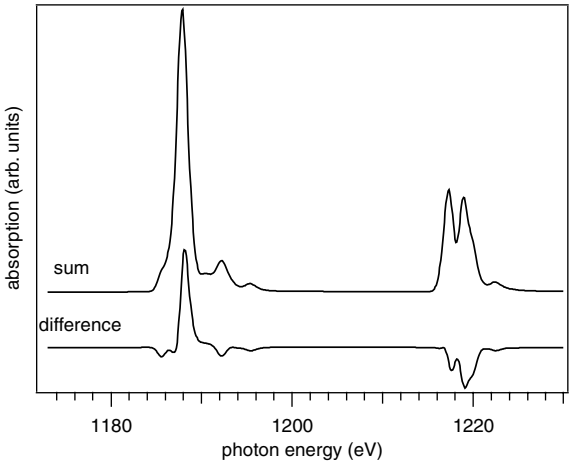

Fig. 3. Results of Hartree-Fock calculations of free Gd^{3+} atoms. Difference and sum spectra are shown. For details see text.

To compare the measured cluster spectra with theory, we performed Hartree-Fock (HF) calculations including relativistic extensions using Cowan's code [42] and the extended Fano theory [43]. A detailed description of the MCD calculations is given in [44,45]. The calculations have been performed on free Gd^{3+} atoms, hereby disregarding the contribution of the $(5d6s)^3$ valence states. The resulting sum and difference spectra are displayed in Figure 3. They clearly show a close resemblance to the measured spectra of the gadolinium samples presented in this work. All the features in the calculations can be found in the measured spectra. Since the spectra are calculated by only taking the $4f$ states into account and no changes to the cluster spectra presented in Figure 2 are observable, the picture of negligible influences of a change in the

valence state configuration on the $3d \rightarrow 4f$ absorption spectra is strengthened.

In the introduction, changes of the average magnetic moments per atom of free clusters were reported in contrast to the unchanged magnetic properties of the f-states shown for deposited monomers and dimers. The magnetic moments of the free cluster atoms are not pinned along a magnetization axis of a substrate and the reduced magnetic moments were thus explained by canted inner-cluster $4f$ spin structures. These canted spin-structures are not likely for the small deposited clusters, as the exchange interaction with the substrate forces the moments into antiparallel alignment and the $4f$ moments remain due to their localization unchanged. A similar result has been obtained for mass selected Cr_n clusters deposited on a magnetized Fe/Cu(100) system [46]. Here for a deposited Cr dimer at first a non collinear magnetic coupling is expected. However, due to the strong coupling to the Fe substrate the Cr_2 cluster is forced into a collinear coupling. Nevertheless, canted spin structures might be important for non-magnetic supports.

These findings are confirmed by XMCD studies of Gd-TM alloys [35,47,48] and by a study of EuSe nanoislands [49]. Here, the shape and the structure of the dichroism spectra are in good accordance with the results presented in this study and no qualitative change is observed. This equality confirms the unchanged magnetic properties of the localized $4f$ electrons in these systems.

As these measurements are on the verge of feasibility, the application of the sum rules [50,51] on the $3d \rightarrow 4f$ XMCD spectra for the determination of spin- and orbital magnetic moments is limited. In the following the difficulties are explained on the basis of the spin moments. The signal to noise ratio is in this energy region due to the low cluster coverage and the low beamline flux small. In addition, an EXAFS wiggle of the Fe/Cu(100) substrate interferes with the $3d_{5/2,3/2}$ resonances, so that a proper background treatment is grievous. In turn, the determination of a proper step function to the sum spectra is impossible.

Therefore, a higher order polynomial was fitted and subtracted from the spectra; an example of this background subtraction is depicted in Figure 2a for a Gd_2 sample. In contrast to the late $3d$ elements (Fe, Co, Ni) the excitation into continuum states is located above the $3d$ resonances. Furthermore the associated step functions are much smaller. Hence, a complicated step function treatment as for the $3d$ elements is not necessary and is already included in our background treatment.

From these spectra the expectation values for the spin and orbital magnetic moments can be extracted by using the sum rules [50,51]

$$\mu_L = 2n_h \frac{\int_{M_5+M_4}(\mu_+ - \mu_-)}{\int_{M_5+M_4}(\mu_+ + \mu_-)}\mu_B$$

$$\mu_S = 2n_h \frac{\int_{M_5}(\mu_+ - \mu_-) - \frac{3}{2}\int_{M_4}(\mu_+ - \mu_-)}{\int_{M_5+M_4}(\mu_+ + \mu_-)}\mu_B + 6\langle T_z\rangle\mu_B.$$

Table 1. Spin and orbital magnetic moments for several Gd and GdO clusters per f-hole. All values are given in units of μ_B. The errors are $\Delta\mu_S = \pm 0.05\ \mu_B$, $\Delta\mu_L = \pm 0.04\ \mu_B$ and ± 0.02 for the ratio.

Cluster	μ_S	μ_L	μ_L/μ_S
Gd_1	0.76	0.10	0.13
Gd_2	0.81	0.10	0.12
Gd_1O	0.80	0.10	0.13
Gd_2O	0.78	0.11	0.14

The results of this sum rule analysis are shown in Table 1. For all clusters the same orbital and spin moments in the order of $\mu_L = 0.10 \pm 0.04\ \mu_B$ and $\mu_S = 0.79 \pm 0.05\ \mu_B$ per f-hole are found. Thus, per Gd atom a total magnetic moment of $6.2 \pm 0.4\ \mu_B$ is found. This value is close to the value of $6.53\ \mu_B$, which is found for the free gadolinium atom. In the atom the reduction of the total moment from the value expected for the half-filled $4f$ shell is due to the coupling of the $4f^7$ electrons with the $5d$ electron. However, in our XMCD experiments only the $4f$ electrons are probed. Hence the reduced moment and the non-zero orbital contribution is somewhat surprisingly.

The application of sum rules to the $4f$ elements is not as straightforward, as for the late $3d$ elements, as has been shown e.g. by Ankudinov et al. [52] for the $5d$ electrons in Tb. Thus, for the absolute values of the magnetic moments one has to add a systematic error. Nevertheless, this error should not change strongly with the cluster size, so the magnetic moments of the different cluster sizes can still be compared.

Let's now focus on the results of the $4d \rightarrow 4f$ absorption. In Figure 4a, XA spectra of the gadolinium monomer measured with circular polarized light (XMCD) are presented. The typical gadolinium $4d \rightarrow 4f$ "giant resonance" is found, accompanied by pre-threshold multiplets in the lower photon energy region. Due to the large photoionization cross section and a much higher photon flux of the beamline in this energy region, the signal to noise ratio of the $4d \rightarrow 4f$ absorption spectra is significantly enhanced compared to the $3d \rightarrow 4f$ spectra.

The giant resonances have their origin in the competition between a direct and an indirect photo excitation process. The direct photoemission $4f^n \rightarrow 4f^{n-1}\epsilon l$ channel hereby quantum mechanically interferes with the indirect channel $4f^n \rightarrow 4d^9 4f^{n+1} \xrightarrow{\text{SCK}} 4f^{n-1}\epsilon l$, whose $4d^9 4f^{n+1}$ intermediate state decays through a Super Coster-Kronig (SCK) Auger decay into the same final state as the one of the direct photoemission channel. The resulting peak profile can be described using the theory of Fano [53].

XMCD spectra of the gadolinium $4d \rightarrow 4f$ giant resonances have been measured for the monomer, dimer and their monoxides deposited onto the iron substrate. Qualitatively, no size dependence is found in the absorption spectra of the monomer and dimer preparations, i.e. the giant $4d \rightarrow 4f$ resonance and the maxima of the pre-edge multiplet structure are found in all clusters. XMCD spectra of thin gadolinium films measured by Starke et al. [40]

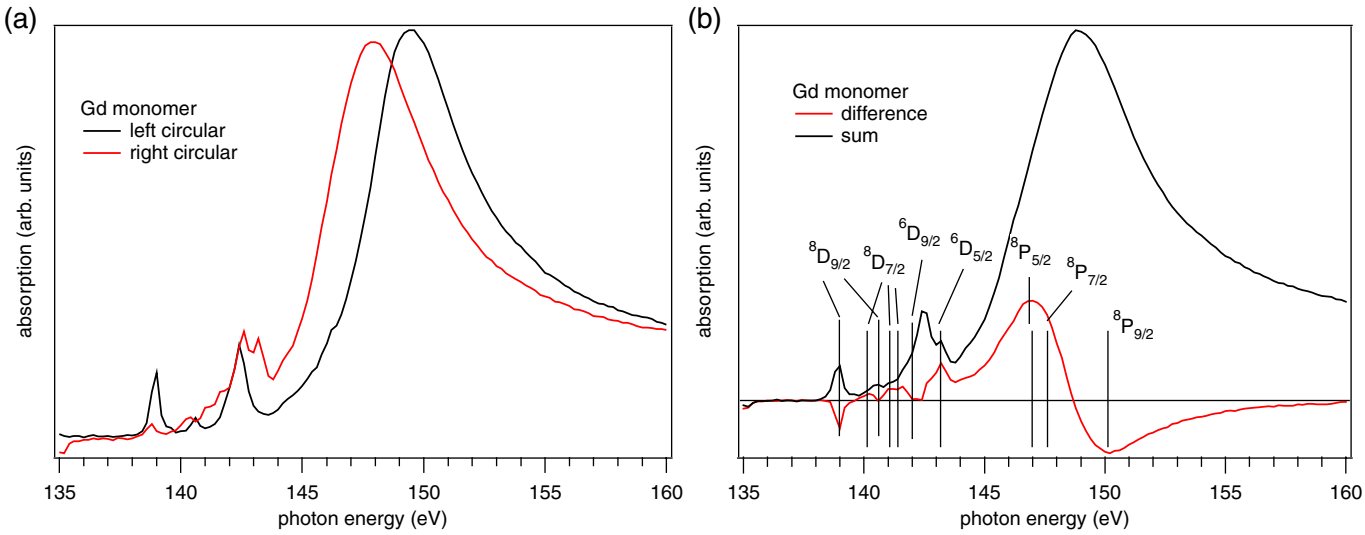

Fig. 4. (Color online) (a) $4d \rightarrow 4f$ X-ray absorption spectra measured with circular polarized light (XMCD) of a gadolinium monomer preparation. (b) Corresponding difference and sum spectra. The allocation of the multiplets is taken from [40].

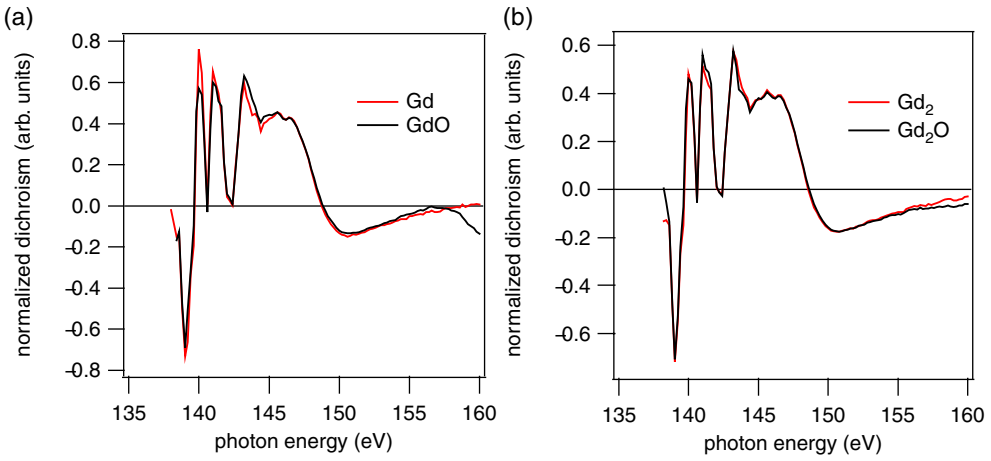

Fig. 5. (Color online) Spectra of normalized dichroism of the (a) gadolinium monomer and its monoxide preparations (b) gadolinium dimer and its monoxide preparations.

are comparable in its shape and no qualitative difference between cluster and thin film spectra is present.

To gain deeper insight in the magnetic properties of these samples, difference and sum spectra are generated. Figure 4b shows, as an example, the resulting spectra for the monomer. Magnetic ordering of the clusters is achieved due to the exchange interaction with the iron substrate, as described above. Magnetic order results in a nonzero difference spectrum. Both, the giant resonance as well as the pre-peak multiplets contribute to the dichroic signal in the difference spectrum. The assignment of the multiplets, as presented in Figure 4b, is taken from Starke et al. [40]. As reported before [40], the states with angular momentum $J = 9/2$ contribute with negative sign to the difference spectra, whereas states with angular momentum $J = 7/2$, $5/2$ with positive sign. The comparison of the cluster spectra with spectra of thin films [40] show, that all peaks are reproduced in the difference spectra of the clusters.

To visualize differences in the spectra of the various cluster preparations, normalized dichroism spectra are gained by the division of the difference spectra by the corresponding sum spectra. The normalized dichroism is an entity being determined with high accuracy, because many factors affecting the dichroic signal, like e.g. insufficient background correction and nonlinearities, cancel due to the normalization out. Figure 5a shows the normalized dichroism spectra of the monomer and monomer monoxide preparations, Figure 5b the dimer and dimer monoxide spectra. Within the statistical limits, no difference between the spectra of the pure clusters and their monoxides is found. In consequence, average spectra consisting of the cluster and monoxide spectra have been generated for the monomer and dimer preparations, separately. For comparison with gadolinium bulk and calculations of free gadolinium atoms, the results of the measurements and calculcations of Starke et al. [40] have been used to determine the corresponding normalized dichroism. Figure 6 contains the average spectra of the normalized dichroism of the monomer and dimer preparations as well as the results of thin films and the free atoms calculation. The spectra presented are set to one at an excitation energy of 146.6 eV, to visualize changes in the relative peak intensities

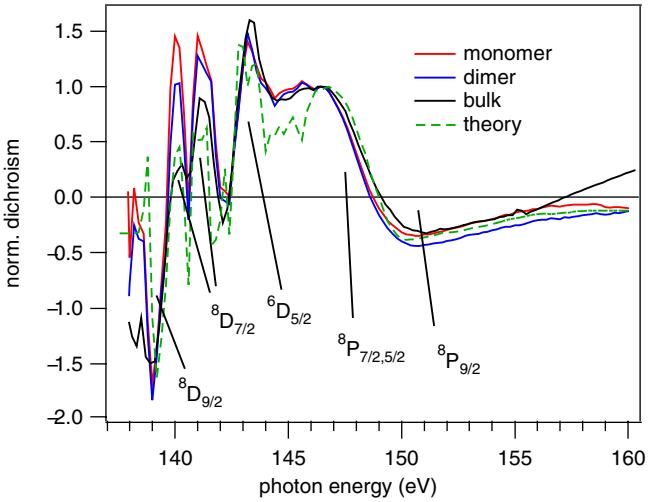

Fig. 6. (Color online) Average normalized dichroism spectra of the monomer and dimer. Bulk and theory spectra are taken from [40]. To visualize relative intensity changes, all spectra have been normalized to one at an arbitrarily chosen photon energy of 146.6 eV.

and cancel differences in the magnetization of the iron substrate.

The comparison clearly shows a close similarity between the spectra of the cluster, the thin film and the free atoms calculation. This is an expected behavior, as the $4d$ electrons are excited into localized $4f$ states, as discussed before. Despite of these findings, multiplets with an angular momentum $J = 7/2$ ($^8D_{7/2}$) show a strong size dependence. The strongest deviation with cluster size is apparently observed for transitions with $\Delta J = 0$, as the gadolinium ground state is $^8S_{7/2}$. The deviation from the bulk values is strongest for the monomer, thereby reflecting a transition from atomic-like towards bulk-like behavior. But why do we observe a size dependent change of the intensities at all? The answer can be found in the comparison of gadolinium with europium $4d \rightarrow 4f$ dichroism spectra. Ogasawara et al. [54] performed calculations of gadolinium and europium $4d \rightarrow 4f$ absorption spectra. The calculated spectra show small deviations between europium and gadolinium in the intensity ratios of the pre-edge multiplet structure. Muto et al. [55] have measured bulk-like europium and gadolinium $4d \rightarrow 4f$ XMCD spectra, showing small changes between gadolinium and europium in the multiplet structure, which are visible despite the low signal to noise ratio in the europium spectra. As discussed above, the difference between gadolinium and europium is in the d-electron count. In contrast to the localized character of the $4f$ states, the gadolinium $5d$ electrons are expected to be strongly influenced by the environment of the atom. In particular, the $5d$ density of states delocalizes with rising cluster size. This effect is well-known from previous experiments on $3d$ TM systems and has been shown for small deposited chromium clusters [41]. Therefore electronic properties of the gadolinium $5d$ electrons are expected to be strongly site dependent (cluster size, oxidation state). When going from an atom towards bulk like structures, the $5d$ electron of gadolinium strongly delocalizes with increasing cluster size and the d-electron count at the atomic site is reduced. Therefore, a change in the d-electron count at the atomic gadolinium site is a change qualitatively comparable with the difference between Eu and Gd. The observed change in the relative intensities in the normalized dichroism can thus be explained by differences in the delocalization of the gadolinium $5d$ electron. Surprisingly this effect seems to be larger for the transition from atom to dimer as compared to Gd atom and GdO.

4 Conclusions

Gadolinium monomers, dimers and their monoxides have been deposited and measured onto ultrathin magnetized iron films using XMCD spectroscopy. An antiferromagnetic coupling of the $4f$ magnetic moments is, consistently with previous findings, for all prepared samples observed. No change between different cluster sizes and their monoxides is found for the $3d \rightarrow 4f$ resonances with in limitations of this experiment, fortifying the picture of localized $4f$ states.

The $4d \rightarrow 4f$ absorption structure shows also no qualitative change of the spectral shape when going from the monomer to the dimer. Additionally, the monoxide formation induces no changes in the $4d \rightarrow 4f$ XMCD spectra. This can be explained by the strong gadolinium-substrate interaction, which dominated the system, therefore, avoiding canted spin alignments.

However, a variation of the relative peak intensities is found for the pre peak structure of the $4d$ giant resonance and in particular for the $^8D_{7/2}$ multiplet. The strongest size dependence is found for transitions with angular momentum $\Delta J = 0$.

We gratefully acknowledge the traditionally great support of the BESSY staff during beamtime. Thanks for fruitful discussions to Kai Starke. Special thanks for technical support go to H. Meyer and S. Gieschen. This work was supported by the German ministry for education and research (BMBF) under grant KS1 GUB/5 and by the Deutsche Forschungsgemeinschaft DFG Wu207/3-1 within the SPP 1153.

References

1. E. Weschke, H. Ott, E. Schierle, C. Schussler-Langeheine, D.V. Vyalikh, G. Kaindl, V. Leiner, M. Ay, T. Schmitte, H. Zabel, et al., Phys. Rev. Lett. **93**, 157204 (2004)
2. H.E. Nigh, S. Legvold, F.H. Spedding, Phys. Rev. **132**, 1092 (1963)
3. R.J.V. Zee, S. Li, W. Weltner, J. Chem. Phys. **100**, 4010 (1994)
4. D. Weller, S.F. Alvarado, W. Gudat, K. Schröder, M. Campagna, Phys. Rev. Lett. **54**, 1555 (1985)
5. D. Weller, S.F. Alvarado, Phys. Rev. B **37**, 9911 (1988)
6. H. Tang, D. Weller, T.G. Walker, J.C. Scott, C. Chappert, H. Hopster, A.W. Pang, D.S. Dessau, D.P. Pappas, Phys. Rev. Lett. **71**, 444 (1993)

7. A.V. Anisimov, V.D. Borman, A.P. Popov, Phys. Rev. B **49**, 3874 (1994)
8. A.B. Shick, W.E. Pickett, C.S. Fadley, Phys. Rev. B **61**, 9213 (2000)
9. C.S. Arnold, D.P. Pappas, Phys. Rev. Lett. **85**, 5202 (2000)
10. G.A. Mulhollan, K. Garrison, J.L. Erskine, Phys. Rev. Lett. **69**, 3240 (1992)
11. R. Wu, C. Li, A.J. Freeman, C.L. Fu, Phys. Rev. B **44**, 9400 (1991)
12. F. Lopez-Urias, A. Diaz-Ortiz, J.L. Moran-Lopez, Physica B **320**, 185 (2002)
13. D.P. Pappas, A.P. Popov, A.N. Anisimov, B.V. Reddy, S.N. Khanna, Phys. Rev. Lett. **76**, 4332 (1996)
14. V.Z. Cerovski, S.D. Mahanti, S.N. Khanna, Eur. Phys. J. D **10**, 119 (2000)
15. L. Hernandez, C. Pinettes, *Study of the influence of surface anisotropy and lattice structure on the behaviour of a small magnetic cluster*, e-print `arXiv:cond-mat/0304015` v2 (2005)
16. D.C. Douglass, J.P. Bucher, L.A. Bloomfield, Phys. Rev. Lett. **68**, 1774 (1992)
17. D.C. Douglass, A.J. Cox, J.P. Bucher, L.A. Bloomfield, Phys. Rev. B **47**, 12874 (1993), URL `http://link.aps.org/abstract/PRB/v47/p12874`.
18. D. Gerion, A. Hirt, A. Châtelain, Phys. Rev. Lett. **83**, 532 (1999)
19. C.E. Krill, F. Merzog, W. Krauss, R. Birringer, Nanostruct. Mater. **9**, 455 (1997)
20. Z.C. Yan, Y.H. Huang, Y. Zhang, H. Okumura, J.Q. Xiao, S. Stoyanov, V. Skumryev, G.C. Hadjipanayis, C. Nelson, Phys. Rev. B **67**, 054403 (2003)
21. S.H. Aly, J. Magn. Magn. Mat. **222**, 368 (2000)
22. L. Nordström, A. Mavromaras, Europhys. Lett. **49**, 775 (2000)
23. J. Lau, A. Achleitner, W. Wurth, Chem. Phys. Lett. **317**, 269 (2000)
24. J. Lau, H.-U-Ehrke, A. Achleitner, W. Wurth, Low Temp. Phys. **29**, 223 (2003)
25. H. Cheng, U. Landman, Science **260**, 1304 (1993)
26. S. Fedrigo, W. Harbich, J. Buttet, Phys. Rev. B **58**, 7428 (1998)
27. J.T. Lau, A. Achleitner, H.-U. Ehrke, U. Langenbuch, M. Reif, W. Wurth, Rev. Sci. Instr. **76**, 063902 (2005)
28. D. Peterka, A. Enders, G. Haas, K. Kern, Phys. Rev. B **66**, 104411 (2002)
29. J. Giergiel, J. Shen, J. Woltersdorf, A. Kirilyuk, J. Kirschner, Phys. Rev. B **52**, 8528 (1995)
30. D. Schmitz, C. Charton, A. Scholl, C. Carbone, W. Eberhardt, Phys. Rev. B **59**, 4327 (1999)
31. J. Stöhr, *NEXAFS Spectroscopy*, volume 25 of Springer Series in Surface Science (Springer, Berlin Heidelberg New York, 1992)
32. W. Kuch, M. Salvietti, X. Gao, M.-T. Lin, M. Klaua, J. Barthel, C.V. Mohan, J. Kirschner, Phys. Rev. B **58**, 8556 (1998)
33. P. James, O. Eriksson, B. Johansson, I.A. Abrikosov, Phys. Rev. B **59**, 419 (1999)
34. C. Carbone, E. Kisker, Phys. Rev. B **36**, R1280 (1987)
35. T. Hatano, S.-Y. Park, T. Hanyu, T. Miyahara, J. Electron Spectrosc. Relat. Phenom. **78**, 217 (1996)
36. G. Panaccione, P. Torelli, G. Rossi, G. van der Laan, M. Sacchi, F. Sirotti, Phys. Rev. B **58**, R5916 (1998)
37. M.S.S. Brooks, O. Eriksson, B. Johansson, J. Phys.: Condens. Matter **1**, 5861 (1989)
38. B. Johansson, L. Nordström, O. Eriksson, M.S.S. Brooks, Phys. Scr. T **39**, 100 (1991)
39. B. Thole, G. van der Laan, J. Fuggle, G. Sawatzky, R. Karnatak, J.-M. Esteva, Phys. Rev. B **32**, 5107 (1985)
40. K. Starke, E. Navas, E. Arenholz, Z. Hu, L. Baumgarten, G. van der Laan, C.T. Chen, G. Kaindl, Phys. Rev. B **55**, 2672 (1997)
41. M. Reif, L. Glaser, M. Martins, W. Wurth, Phys. Rev. B **72**, 155405 (2005)
42. R.D. Cowan, *The Theory of Atomic Structure and Spectra* (University of California Press, Berkeley, 1981)
43. F.H. Mies, Phys. Rev. **175**, 164 (1968)
44. G. Prümper, S. Kröger, R. Müller, M. Martins, J. Viefhaus, P. Zimmermann, U. Becker, Phys. Rev. A **68**, 032710 (2003)
45. M. Martins, J. Phys. B **34**, 1321 (2001)
46. S. Lounis, M. Reif, P. Mavropoulos, L. Glaser, P.H. Dederichs, M. Martins, S. Blügel, W. Wurth, submitted (2007)
47. M. Mizumaki, K. Yano, I. Umehara, F. Ishikawa, K. Sato, A. Koizumi, N. Sakai, T. Muro, Phys. Rev. B **67**, 132404 (2003)
48. S. Qiao, A. Kimura, H. Adachi, K. Iori, K. Miyamoto, T. Xie, H. Namatame, M. Taniguchi, A. Tanaka, T. Muro, et al., Phys. Rev. B **70**, 134418 (2004)
49. T.U. Schülli, R.T. Lechner, J. Stangl, G. Springholz, G. Bauer, S. Dhesi, P. Bencok, Appl. Phys. Lett. **84**, 2661 (2004)
50. B.T. Thole, P. Carra, F. Sette, G. van der Laan, Phys. Rev. Lett. **68**, 1943 (1992)
51. P. Carra, B.T. Thole, M. Altarelli, X. Wang, Phys. Rev. Lett. **70**, 694 (1993)
52. A. Ankudinov, J. Rehr, H. Wende, A. Scherz K. Baberschke, Europhys. Lett. **66**, 441 (2004)
53. U. Fano, Phys. Rev. **124**, 1866 (1961)
54. H. Ogasawara, A. Kotani, J. Phys. Soc. Jpn **64**, 1394 (1995)
55. S. Muto, S.-Y. Park, S. Imada, K. Yamaguchi, Y. Kagoshima, T. Miyahara, J. Phys. Soc. Jpn **63**, 1179 (1994)